

Evaluating the Merger Rate of Binary Black Holes from Direct Captures and Third-Body Soft Interactions Using the Milky Way Globular Clusters

Konstantinos Kritos^{1,*} and Ilias Cholis^{2,†}

¹*Physics Division, National Technical University of Athens, Zografou, Athens, 15780, Greece*

²*Department of Physics, Oakland University, Rochester, Michigan, 48309, USA*

(Dated: July 8, 2020)

The multitude of binary black hole coalescence detections in gravitational waves has renewed our interest on environments that can be the cradle of these mergers. In this work we study merger rates of binary black holes in globular clusters that are among the most dense stellar environments and a natural place for the creation of black hole binaries. To model these systems with all their variations we rely on the observational properties of the known Milky Way globular clusters. We consider direct capture events between black holes, as well as soft interactions of black hole binaries with stars as third bodies that accelerate the evolution of these binaries. We find that binary black holes from direct captures merge at an averaged rate of $0.3 - 5 \times 10^{-11} \text{ yr}^{-1}$ per cluster. Third body soft interactions are a much more prominent channel giving an averaged rate of $2 - 4 \times 10^{-10} \text{ yr}^{-1}$ per cluster. Those rates in globular clusters can lead to a cumulative merger rate of about 100 mergers per year up to redshift of 1, i.e. a significant fraction of the detectable in the near future binary black hole coalescence events. Further observations of cluster properties both in terms of their masses, profile properties, velocity dispersion of stars and their cosmological distribution, will allow us to better constrain the contribution of these environments to the detectable coalescence events rate.

I. INTRODUCTION

The Laser Interferometer Gravitational wave Observatory (LIGO) [1] with its first three observing runs concluded allows us a first measurement on the rates of binary black hole (BBH) merges in the local Universe [2]; and ask questions on the mechanisms/environments responsible for them [3–23]. Moreover, as LIGO observes more coalescence events, the growing statistics will allow us to address their population synthesis [24–28]. Globular clusters (GCs) are among the systems with the highest densities in stars, and environments where stellar mass objects can undergo multiple dynamical encounters that may lead to merger events [4, 18, 29–33]. Extensive N-body simulations regarding the evolution and interactions of black holes (BH) inside dense star cluster systems have been performed in the past, [32, 34–37]. We utilize this rich dynamics to evaluate merger rates of BBH systems in dense stellar clusters throughout cosmic history. Such clusters may provide an explanation for the origin of an important component of the total merger rate of BH binaries, and also the places where consecutive mergers occur [29, 38–40], that can be probed by current observatories [41–45].

In this article we study mergers of stellar mass BBH systems formed in GCs. We model the mass-distribution of objects in GCs by the sum of two Dirac delta functions. One represents a generic light stellar object of mass $m_{\text{star}} = 1 M_{\odot}$ and the other a typical BH of mass

$m_{\text{BH}} = 10 M_{\odot}$. We will refer to this choice as “two body model”. Their relative weight is determined by the initial stellar mass function. Some of these BHs will participate in binaries. Our choice of mass-distribution allows us to focus on binaries of equal-mass BHs distributed throughout the GCs. Unequal mass ratios are rare in GCs, as strong interactions of the binary with massive third bodies as other BHs lead to the binary exchanging its lighter member with the interacting more massive object. Furthermore, we assume that the stellar population follows that of the GC’s mass density profile with the appropriate normalization. Most of the BHs are concentrated instead at the denser core due to mass segregation that happens in the first $O(10^2)$ Myr of the cluster’s evolution.

We ignore effects as mass loss during the cluster’s evolution as the dynamics of BBHs take place mostly at the inner parts of the cluster’s profile. However, we note that as BBHs interact strongly with individual stars they get on orbits that temporarily move them further away from the GC core and probe a wider volume of the cluster. We find that 3rd-body soft interactions, do not typically eject the BBHs before they are already quite tight after which point they will rapidly merge. While interactions of BHs with stars lead to the depletion of stars from the very center of the GCs, $1 M_{\odot}$ stars are not completely depleted out to the core radius of the GCs.

An isolated binary in the low density field loses energy into gravitational waves (GW) as predicted by the general theory of relativity. This radiation reaction leads to coalescence on a timescale given by [46],

$$T_{gw}(e_0 = 0) \approx 1.58 \times 10^{14} \left(\frac{a_0}{1 \text{ AU}} \right)^4 \left(\frac{10 M_{\odot}}{m} \right)^3 \text{ yr}, \quad (1)$$

* ge16004@central.ntua.gr

† cholis@oakland.edu, ORCID: orcid.org/0000-0002-3805-6478

for a circular binary of equal mass m BHs with initial semi-major axis and eccentricity given by the pair (a_0, e_0) . For widely separated binaries gravitational radiation is an inefficient process to lead to coalescence. However, in dense environments dynamical interactions accelerate the binary's evolution. This can be achieved in various ways and many different channels have been proposed in the literature regarding the coalescence of two BHs, in dense environments, see e.g. [32, 47]. Relevant in this context, mechanisms include direct capture (DC) merger events [48, 49] and the hardening process of a binary via encounters with third bodies, mainly soft third-body interactions [50–53]. For the case of high merger rates this may also lead to runaway growth of intermediate-mass BHs in GCs, [39, 40]. Other type of effects include stable [54] or meta-stable [55] triple resonance systems, which may form as a consequence of multiple-body interactions, [56].

In this work we focus on the two dominant contributing channels to our total merger rate from GCs. We start with the direct capture events and the interactions involving a BBH system and a third object (3rd-body channel). The values describing the GCs' mass, central densities and velocity dispersion of stars span orders of magnitude; which has a strong impact on their respective merger rates. After averaging over the known Milky Way GCs we find that the direct capture merger rate is $0.3 - 5 \times 10^{-11} \text{ yr}^{-1}$ per cluster. Moreover, by evolving the BBHs in the environments of their respective Milky Way GCs, we evaluate the merger rate due to 3rd-body soft interactions to be $2 - 4 \times 10^{-10} \text{ yr}^{-1}$ per cluster. The rates for the 3rd-body channel are directly proportional to the fraction of BHs that will remain in the cluster and form BBHs hard enough to survive their first encounters with stars. The ratio of the number of these BBHs to the number of the total BHs created from stellar evolution is taken to be 0.3%.

This paper is constructed as follows. In section II we discuss our assumptions on the globular cluster properties and the abundance of BHs in them. We also show our methodology for calculating the BBH merger rates from direct capture events and from third-body hardening processes. In section III, we first present results for our example globular cluster 47 Tuc. We then expand our results to a sample of 13 Milky Way GCs that encompass the variations between those environments; and then include the contribution from all Milky Way globular clusters that we have information for. Using the Milky Way clusters as a representative sample for all clusters of the local Universe we then evaluate their BBH cosmological merger rate. Finally, in section IV we give our conclusions.

II. ASSUMPTIONS AND METHODOLOGY

A. The mass profile of globular clusters

We take Milky Way GCs that have relatively well observed mass distributions, with that information publicly available at [57]. As a reference we assume that the mass distribution of stars $\rho(r)$ in GCs follows a King profile, [58],

$$\rho_{\text{King}}(r) = \rho_0 \left[\frac{\left(1 + \left(\frac{r}{r_c}\right)^2\right)^{-\frac{1}{2}} - (1 + 100c)^{-\frac{1}{2}}}{1 - (1 + 100c)^{-\frac{1}{2}}} \right]^2, \quad (2)$$

with ρ_0 the central density $\rho_{\text{King}}(r=0)$. The core radius r_c and the concentration parameter c are related to the tidal radius r_t of the GC via $c = \log_{10}(r_t/r_c)$. We rely on Ref. [57] for the particular values of individual GCs. The mass of each of these clusters is calculated by integrating their density out to their tidal radius,

$$M_{GC} = \int_0^{r_t} dr 4\pi r^2 \rho_{\text{King}}(r). \quad (3)$$

For the BHs that are in the GC, mass segregation takes place leading to BHs concentrating near the center of each GC. We assume for simplicity that all BHs are uniformly distributed within the core radius. The exact profile of the BHs' density is a detail as our final rates will prove to depend mostly on the total number of BHs and BBHs per cluster.

The velocity dispersion of the stars in the cluster can be calculated by applying the Virial theorem [59],

$$\sigma(r) = \sqrt{\frac{2GM(r)}{r}}, \quad (4)$$

where G is Newton's constant and $M(r)$ is the total mass contained within a sphere of radius r centered at the center of the GC. The dynamics of the GC are characterized by the relaxation timescale ($O(10^2)$ Myr for BHs).

As an alternative profile for the stars in GCs we take a Plummer model [60],

$$\rho_{\text{Plummer}}(r) = \frac{3 M_{GC}}{4\pi r_{pl}^3} \left[1 + \left(\frac{r}{r_{pl}}\right)^2 \right]^{-\frac{5}{2}}, \quad (5)$$

where $r_{pl} = \frac{r_c}{\sqrt{\sqrt{2}-1}} \approx 1.554r_c$ (Eq. 38 from [61]) is a characteristic parameter called the Plummer radius. We ensure that M_{GC} for each cluster is the same regardless of their mass profile ¹.

¹ Only up to 3% of the mass of a GC is in BHs and thus M_{GC} is accurate for the mass in the stars.

The velocity dispersion is given by, [61],

$$\sigma_{\text{Plummer}}^2(r) = \frac{GM_{GC}}{6\sqrt{r^2 + r_{pl}^2}}. \quad (6)$$

In Table I we show the profile properties for 13 Milky Way GCs. These constitute a representative sample of how much different clusters can contribute to our final results on the merger rate.

GC	$\frac{r_c}{1\text{pc}}$	c	$\frac{r_{pl}}{1\text{pc}}$	$\log_{10}\left(\frac{\rho_0}{1M_\odot/\text{pc}^3}\right)$	$\frac{M_{GC}}{10^5 M_\odot}$	$N_{BH}^{\text{ret-max}}$
47 Tuc	0.47	2.07	0.73	4.88	38.2	1145
ω Cen	3.60	1.31	5.57	3.15	49.3	1477
M15	0.42	2.29	0.66	5.05	68.7	2060
M22	1.24	1.38	1.92	3.63	7.30	219
NGC 6362	2.50	1.09	3.88	2.29	1.29	38
NGC 5946	0.25	2.50	0.38	4.68	9.44	283
M 30	0.14	2.50	0.22	5.01	3.80	113
Terzan 5	0.32	1.62	0.50	5.14	7.51	225
Pal 2	1.35	1.53	2.09	4.06	36.8	1103
NGC 6139	0.44	1.86	0.69	4.67	11.7	351
NGC 2808	0.70	1.56	1.08	4.66	22.1	661
NGC 5286	0.95	1.41	1.48	4.10	10.6	319
NGC 6316	0.51	1.65	0.80	4.23	4.08	122

TABLE I. The parameters of 13 Milky Way GCs relevant in our calculations. The information for the second, third and fifth columns is from Ref. [62]. For the last column we have used $N_{BH}^{\text{ret-max}} = \left(\frac{f_{\text{ret}}}{0.1}\right) N_{BH}^{\text{max}}$ and a BH mass fraction f_{BH} of 0.03 (see Eqs 7 and 8).

In Fig. 1 we give the profiles of $\rho(r)$ and $\sigma(r)$ for three Milky Way GCs.

B. Black holes inside globular clusters

Assuming that stars with mass \mathcal{M} larger than $25 M_\odot$ necessarily give a BH within a few 10^6 yr, and that about 1/3 of the star's original mass is retained by the resulting BH, we can estimate the mass fraction of the GC that ends up in BHs,

$$f_{BH} \simeq \frac{1}{3} \frac{1}{M_{GC}} \int_{25M_\odot}^{120M_\odot} d\mathcal{M} \mathcal{M} \xi(\mathcal{M}) \approx 0.03, \quad (7)$$

where $\xi(\mathcal{M})$ is the Kroupa initial mass function, for which we take the central values of [63]. Taking all BHs to have a mass of $10 M_\odot$, we can estimate their maximum number in a GC to be,

$$N_{BH}^{\text{max}} = f_{BH} \frac{M_{GC}}{10 M_\odot}. \quad (8)$$

As BHs have natal kicks only a fraction, f_{ret} , of them is retained in the cluster. The maximum retained number of BHs in the cluster is,

$$N_{BH}^{\text{ret-max}} = f_{\text{ret}} \times N_{BH}^{\text{max}}. \quad (9)$$

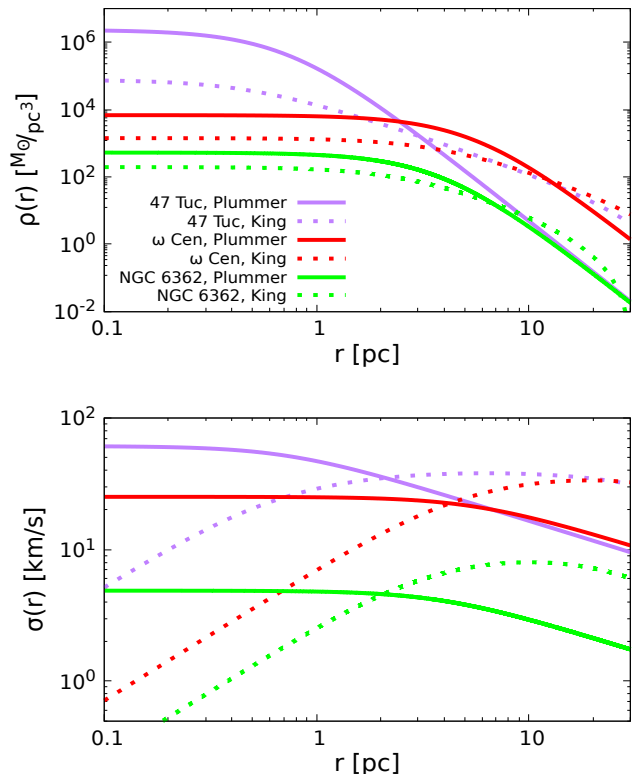


FIG. 1. The profiles of mass density and velocity dispersion for 47 Tuc, ω Cen and NGC 6362. Solid lines represent the Plummer and dashed ones the King model.

Numerical N-body surveys and analytic considerations point out to a value of about $f_{\text{ret}} \simeq 10\%$ up to the tidal radius, consistent with a total mass of $M_{GC} \approx 10^5 M_\odot$, virial radius of $r_v = 1$ pc and $\sigma_{BH} = 50$ km/s, [37] (see also [64, 65]).

Our choice of parameters above allows us to assume energy equipartition between the BH population and their surrounding stars. The Spitzer's criterion in our case is satisfied, as $f_{BH} \times f_{\text{ret}} \times (m_{BH}/1 M_\odot)^{1.5} \simeq 0.1$ and smaller than 0.16, valid for the two-mass model of the GCs that we consider here [66]. Thus, the subsystem of BHs that forms due to mass segregation in our GCs is not dynamically decoupled from that of stars.

Some of these BHs will be in binaries while most of them will be isolated. Consider a Keplerian BBH defined by its orbital semi-major axis and eccentricity parameters (a, e) and with binding energy $E_{\text{bin}} \equiv \frac{G m^2}{2a}$. Then, this binary is said to be hard if its binding energy well exceeds the kinetic energy (KE) of its neighboring objects [67]. When the above condition is not met we will refer to the binaries as soft. BH binaries that originate from binary stars i.e. survived both natal kicks and did not lead to a soft binary that would break with third body

interactions are defined here as proto-BBH (PBBH)². We include into the PBBHs, binaries that were created by exchange interactions of BH-star binaries with an isolated BH. Some of these isolated BHs may form binaries with ordinary stars via three body induced interactions at a high rate, [69], or from a BH sub-population near the core, resulting in the development of a binary population of dynamically assembled BHs, [36].

The maximum total number of BHs in the GC given in Eq. 8 can be decomposed into those that begin in isolation, and those that initially participate into binaries,

$$N_{BH}^{\text{ret-max}} = N_{BH,\text{isol}} + N_{BH,\text{bin}}. \quad (10)$$

In turn the number of PBBHs is,

$$\begin{aligned} N_{\text{PBBH}} &= \frac{1}{2} \times f_{\text{hard}} \times N_{BH,\text{bin}} \\ &= \frac{1}{2} \times f_{\text{hard}} \times \left(\frac{N_{BH,\text{bin}}}{N_{BH}^{\text{ret-max}}} \right) N_{BH}^{\text{ret-max}} \\ &= \frac{1}{2} \times f_{\text{hard}} \times f_{\text{bin}} \times N_{BH}^{\text{ret-max}}. \end{aligned} \quad (11)$$

f_{bin} refers to the fraction of BHs in binaries. Since only hard binaries will make it “unscathed” from early interactions with neighboring bodies, only a fraction f_{hard} of binaries will be our PBBHs. Those may eventually merge after further hardening 3rd-body interactions.

Combining with Eq. 9 we get,

$$\begin{aligned} N_{\text{PBBH}} &= \frac{1}{2} \times f_{\text{hard}} \times f_{\text{bin}} \times f_{\text{ret}} \times N_{BH}^{\text{max}} \\ &= f_{\text{eff}} \times N_{BH}^{\text{max}}. \end{aligned} \quad (12)$$

where we have combined all previously mentioned factors into a single effective factor $f_{\text{eff}} \equiv 1/2 \times f_{\text{hard}} \times f_{\text{bin}} \times f_{\text{ret}}$. From this point on when discussing the 3rd-body channel we will only care about the PBBHs’ evolution and refer to these binaries as just BBHs.

Monte Carlo simulations from [7, 29] that study BBHs in clusters and probe the $f_{\text{eff}}/f_{\text{ret}}$ ratio, suggest a range of $0.01 \lesssim f_{\text{eff}}/f_{\text{ret}} \lesssim 0.1$. Since we take $f_{\text{ret}} \simeq 0.1$ we will consider the range for the effective factor to be $1 \times 10^{-3} \lesssim f_{\text{eff}} \lesssim 1 \times 10^{-2}$.

The remaining isolated BHs may contribute to the DC channel or participate in hard binaries³. Their number is $(1 - f_{\text{hard}} \times f_{\text{bin}}) \times f_{\text{ret}} \times N_{BH}^{\text{max}} \simeq f_{\text{ret}} \times N_{BH}^{\text{max}}$.

C. The merger rate

Assuming that the GC properties depend only on the radial distance from the center, and ignoring mass distri-

butions, we can write a universal scheme for the differential merger rate in the GC regarding a single merger channel as,

$$\frac{d\Gamma_{\text{ch.}}}{d^3r} = n_{\text{ch.}}(r) \left\langle \frac{1}{T_m(r)} \right\rangle. \quad (13)$$

Here, $n_{\text{ch.}}$ is the number density of merger events in that channel and $\langle \frac{1}{T_m(r)} \rangle$ is the average rate for such an event at radius r . In the following we will apply this formula in the cases of the DC channel and the 3rd-body channel, as these are the dominant contributing channels to our total merger rate from GCs. For an N-object configuration with $N \geq 3$ the probability for interaction gets significantly suppressed with increasing N.

1. Direct Capture events

In [48, 71] the cross section for the DC channel is calculated assuming that a pair of objects A and B , with reduced mass μ_{AB} , can form a bound system as long as they interact at such a small pericenter so that the energy lost in GWs exceeds the total energy of the reduced system; i.e. $\delta E_{GW} \geq \frac{1}{2} \mu_{AB} \sigma_{AB}^2$, where $\sigma_{AB} = \sqrt{1 M_{\odot} / \mu_{AB}} \sigma_{\text{star}}$ since we have assumed energy equipartition. δE_{GW} was calculated in [72]. σ_{star} is the velocity dispersion of the stars as shown in Fig. 1. The cross section for this interaction is,

$$\begin{aligned} \Sigma_{DC} &\simeq 16.8 \times \left(\frac{\sigma_{AB}}{c} \right)^{-18/7} \\ &\times \left(\frac{G^2 m_A^{2/7} m_B^{2/7} (m_A + m_B)^{10/7}}{c^4} \right), \end{aligned} \quad (14)$$

in the gravitational focusing approximation and under the hypothesis that $A - B$ interactions are nearly parabolic, [48]. In this work we care for both A and B to be $10 M_{\odot}$ BHs. The total DC merger rate over a GC, is just,

$$\Gamma_{DC} = \int_{r_{\text{min}}}^{r_{\text{max}}} dr 4\pi r^2 \frac{1}{2} n_{BH}^2 \Sigma_{DC} v_{BH,BH}. \quad (15)$$

We take for the relative velocity of two BHs $v_{BH,BH} = \sigma_{BH,BH} = \sqrt{2} \sigma_{BH}$; σ_{BH} is the velocity dispersion of the BHs.

In our calculations we use a lower limit of radius r_{min} ,

$$r_{\text{min}} = \left(\frac{4\pi}{3} n_{BH}^{\text{ret-max}}(r=0) \right)^{-1/3}, \quad (16)$$

i.e down to the radius where only one $10 M_{\odot}$ BH is included. We also take $r_{\text{max}} = r_c$, as we assume all BHs within the core radius.

Every DC event leads to a merger as the timescale for isolated radiation reaction coalescence is very small compared to the interaction timescale with an object that

² Also known in the literature as “primordial binaries”, see e.g. [68]

³ There may be soft binaries that survive and contribute to the 3rd-body channel. The disruption of hard binaries due to some very energetic interaction giving off two isolated BHs is a rare event, [67, 70].

might disturb the BH binary. The merger timescale for a newly DC-formed BBH is bounded above by, [73, 74],

$$T_m^{DC} \lesssim 376 \times \left(\frac{m_{BH}}{10 M_\odot} \right) \times \left(\frac{10 \text{ km/s}}{\sigma_{\text{star}}} \right)^3 \text{ yr.} \quad (17)$$

The interaction timescale in our context is given by,

$$T_{\text{int}} = 15.6 \times \left(\frac{\sigma_{\text{star}}}{10 \text{ km/s}} \right) \times \left(\frac{0.4 \times 10^5 M_\odot / \text{pc}^3}{\rho_{\text{star}}} \right) \times \left(\frac{20 M_\odot}{m_{\text{tot}}} \right) \times \left(\frac{6 \text{ AU}}{a_h} \right) \text{ Myr,} \quad (18)$$

which is much larger than T_m^{DC} .

2. 3rd-body hardening process on BBH

A hard circular BBH with SMA of 0.1 AU or larger will merge on a timescale that is larger than the Hubble time (Eq.1). However, interactions of the binary with stars can lead to the hardening of the BBH, with the stars gaining kinetic energy out of the binary and thus increasing its binding energy. A few 3rd-body interactions inside of dense stellar clusters may be enough to accelerate the merger [67, 70].

We take a hard semi-major axis to be defined by, ⁴ [75],

$$a_h = \frac{G m_{BH}}{4 \sigma^2} \simeq 5.58 \times \left(\frac{m_{BH}}{10 M_\odot} \right) \left(\frac{20 \text{ km/s}}{\sigma_{\text{star}}} \right)^2 \text{ AU.} \quad (19)$$

Considering an energetic interaction with a point of closest approach of the order of the binary's semi-major axis, i.e. $\sim a$, the average fractional energy variation per encounter is given by,

$$\frac{\langle \Delta E_b \rangle}{E_b} \simeq 0.12 \times \left(\frac{H}{15} \right) \left(\frac{m_{\text{star}}}{1 M_\odot} \right) \left(\frac{10 M_\odot}{m_{BH}} \right). \quad (20)$$

H is the hardening rate (not to be confused with the Hubble rate), [75]. H is best determined by numerical 3rd-body experiments, as in [76], where it was approximated by,

$$H = 14.55 \times \left(1 + 0.287 \frac{a}{a_h} \right)^{-0.95}, \quad (21)$$

for a unit mass ratio BBH and independent of e^5 . Furthermore, we use an averaged time rate of change of the

binary's internal energy is given by⁶,

$$\left\langle \dot{E}_b \right\rangle = \langle \Delta E_b \rangle n_{\text{star}} \pi b^2 \sigma_{\text{rel}}, \quad (22)$$

where the impact parameter can be shown to be, [77], $b^2 = r_p^2 \left(1 + \frac{2Gm_{\text{tot}}}{r_p \sigma_{\text{rel}}} \right)$, with a relative velocity of $\sigma_{\text{rel}} \simeq \sigma_{\text{star}}$.

The effective merger timescale can be estimated from the evolution of the semi-major axis alongside with that of eccentricity. The total semi-major axis evolution is given by,

$$\dot{a} = - \frac{G H \rho_{\text{star}}}{\sigma_{\text{star}}} a^2 - \frac{128}{5} \frac{G^3 m_{BH}^3}{c^5 a^3} F(e). \quad (23)$$

The first term describes the averaged effect of hardening interactions while the second term is the Peters secular evolution due to GW emission [46]. $F(e)$ is given by,

$$F(e) = (1 - e^2)^{-7/2} \cdot \left(1 + \frac{73}{24} e^2 + \frac{37}{96} e^4 \right) \text{ for } e \in [0, 1]. \quad (24)$$

Similarly the eccentricity evolution equation is, [76, 78],

$$\dot{e} = + \frac{G H K \rho_{\text{star}}}{\sigma_{\text{star}}} a - \frac{608}{15} \frac{G^3 m_{BH}^3}{c^5 a^4} D(e). \quad (25)$$

K is called the ‘‘eccentricity growth rate’’, [75] which is also determined by numerical 3rd-body experiments. We use the fitting function provided in [76] (their equation 18). The second term in Eq. 25 represents the GW Peters secular evolution of the eccentricity with $D(e) = (1 - e^2)^{-5/2} \cdot \left(e + \frac{121}{304} e^3 \right)$, [46]. We solve the differential system of equations 23 and 25 for a hard binary and for a few pairs of initial conditions (a_0, e_0) . We use as reference 47 Tucanae or just 47 Tuc (NGC 104) at its core radius and later on expand our analysis on other clusters.

The merger for the 3rd-body channel is calculated from,

$$\Gamma_{\text{3rd-body}} = f_{\text{eff}} \times f_{BH} \times \int_{r_{\text{min}}}^{r_{\text{max}}} dr 4\pi r^2 \frac{\rho(r)}{m_{BH}} \frac{1}{T_{GC}} \langle f_e(r) \rangle, \quad (26)$$

where we have used $n_{\text{3rd-body}} = N_{\text{PBH}} \rho(r) M_{GC}^{-1}$. $\rho(r)$ is the mass density of the cluster and $\simeq \rho_{\text{star}}(r)$. T_{GC} is the age of the cluster and f_e refers to the fraction of BBHs that will merge within a time of T_{GC} and obtained by evolving Eqs 23 and 25 for a hard BBH. In our case this reduces to $\Gamma_{\text{3rd-body}} = f_{\text{eff}} \times N_{BH}^{\text{max}} \times \langle f_e(r_c) \rangle / T_{GC}$.

III. RESULTS

We use equations 15 and 26 to calculate the DC and 3rd-body merger rates for the Milky Way GCs.

⁴ The definition of a hard binary of Eq. 19 corresponds to setting its semimajor axis a factor of $\sim 0.025 \times \left(\frac{m_{\text{star}}}{1 M_\odot} \right) \left(\frac{10 M_\odot}{m_{BH}} \right)$ to match Ref. [75]. This is smaller than the value of semi-major axis evaluated by setting $\frac{G m_{BH}^2}{2a} \simeq \frac{1}{2} m_{\text{star}} \sigma_{\text{star}}^2$.

⁵ There is a weak dependence of H on the eccentricity. The coefficient at Eq. 21 varies from 14.5 at $e = 0$ to 17 at $e = 0.9$.

⁶ The over-dot denotes time derivative.

A. The Merger Timescale of Binary Black Holes in 47 Tuc; our example cluster

We start with the BBH evolution on a single cluster to show our treatment of these objects near the GC core. We use 47 Tuc as reference.

1. The Averaged Direct Capture Merger Timescale

We know that the interaction timescale of two objects inside a dense environment depends on their number densities, their relative velocity, as well as their impact parameter. We assume that the typical relative velocity of two BHs is just $\sqrt{2}\sigma_{BH}$, with σ_{BH} their velocity dispersion. Relying on Eq. 14 we can estimate the time required for a $10 M_{\odot}$ BH to interact with a $10 M_{\odot}$ and lead to a DC event. For future reference, we call this time T_{DC} . It is approximately equal to,

$$T_{DC} \simeq 8.2 \times 10^{13} \cdot \left(\frac{100 \text{ pc}^{-3}}{n_{BH}^{\text{ret-max}}(r)} \right) \left(\frac{\sigma_{\text{star}}(r)}{10 \text{ km/s}} \right)^{11/7} \times \left(\frac{10 M_{\odot}}{m_{BH}} \right)^2 \text{ yr.} \quad (27)$$

We take the velocity dispersion of the BHs to be that of the stars multiplied by the factor of $1/\sqrt{10}$ assuming energy equipartition⁷. Mass segregation will also result in lower velocity dispersion for the BHs. Our choice gives an upper bound on the T_{DC} , which in turn will give a lower/conservative limit for the merger rate for this channel. Also, in our case, $n_{BH}^{\text{ret-max}} \simeq \left(\frac{4}{3}\pi r_c^3 \right)^{-1} N_{BH}^{\text{ret-max}}$.

In the case of 47 Tuc, we calculate this time near the center of the GC at the core radius, where most of the BHs reside. We find that such a BH encounters another BH in about 4.7×10^{13} yr according to the Plummer model, and in about 0.9×10^{13} yr in the King model. The Plummer timescale is only slightly bigger than the King one, due to its higher velocity dispersion, (see Fig. 1). Both of these timescales are larger than the Hubble time in the case of 47 Tuc, which indicates DC are rare events inside of 47 Tuc alike GCs. However these numbers are to be understood as averages and the probability that a BH encounters another BH follows the Poisson distribution.

2. The BBH Merger Timescale due to 3rd-body interactions

For the BBH interactions with stars, we solve Eqs. 23 and 25 numerically. Our results are to be understood in a statistical sense and as we show later the evolution

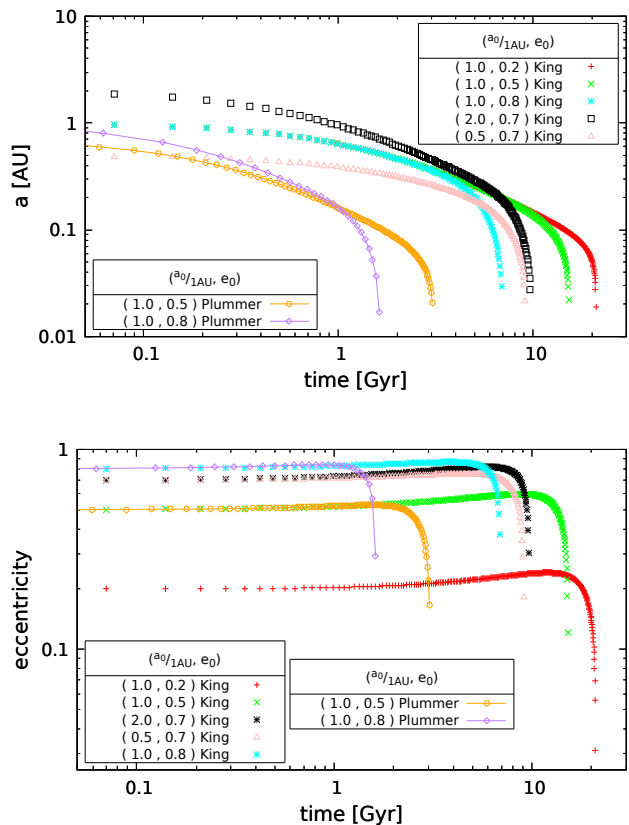


FIG. 2. The evolution of a hard BBH in 47 Tuc at its core radius. The red (plus) and green (cross) overlap with the cyan (star) SMA data because they have the same evolution until 5 Gyr. The black (square) and pink (triangle) data have approximately the same merger times even though their initial semi-major axis differs by a factor of four. We also include two curves, the purple (diamonds) and orange (hexagonal) data, that correspond to a Plummer profile.

of BBHs depends on the specific environment defined by the mass profile of the clusters.

Let us consider a BBH in the environment of 47 Tuc, at core radius. For illustrative purposes at first we ignore the variation of the binary's radius from the center of the GC and study its evolution for a few pairs of initial conditions (a_0, e_0) . We solve the system of equations (23) and (25) implementing a fourth-order Runge-Kutta type numerical algorithm and iterate until the BBH attains a semi-major axis of $a_{\text{end}} = 0.01$ AU. For the time-step we choose $dt = 30$ Myr which is the typical timescale for 3rd-body interactions at the core of 47 Tuc (see appendix A for further details).

In Fig. 2 we show the evolution of BBHs undergoing 3rd-body interactions with starts starting from different (a_0, e_0) conditions. We show five simulations under the assumption of a King density profile and two simulations under a Plummer profile.

In the binary's early evolution, the positive sign of the first term in Eq. 25 (relating to the 3rd-body hardening

⁷ The velocity dispersion of BHs in the inner sub-cluster is expected to be at around 14.5 km/s for 47 Tuc, as is predicted by the Virial theorem at core radius and neglecting the mass contribution from the stars.

interactions) dominates⁸. As a result the eccentricity of the BBH increases at first. That increased eccentricity in turn enhances the GW emission, which accelerates the binary’s coalescence. Throughout the binary’s evolution, both the GW emission and the 3rd-body interactions cause a reduction of the semi-major axis of the binary (Eq. 23). As a becomes smaller the binary’s interactions with stars become more separated in time, suppressing the positive \dot{e} first term in Eq. 25; while the GW emission becomes more prominent, amplifying the negative \dot{e} second term in Eq. 25. At some point the binary enters the GW domination regime, leading to the coalescence and circularization of the binary.

For a BBH in a Plummer environment the merger timescale is smaller compared to a King type core. The ratio ρ/σ in the Plummer profile is larger by about one order of magnitude enhancing the first term in Eq. 23 which drives the binary to shrink more efficiently. This also translates to a larger 3rd-body merger rate for the Plummer profile compared to the King one.

Given that GCs have ages up to $\simeq 10$ Gyr, any of our simulated BBHs that require more than that time to coalesce can not contribute to the BBH merger rates. For a given GC environment, that upper limit on T_m constrains the combination of initial BBH properties (a_0, e_0) required for a binary to merge (within 10 Gyr).

In Fig. 3, we show for combinations of (a_0, e_0) the 3rd-body interactions merger timescale versus the dimensionless semi-major axis a_0/a_h . Every symbol represents the T_m for a unique set of initial conditions. Any point inside the yellow region satisfies $T_m < 10$ Gyr, and its y -axis value gives the predicted T_m . In Fig. 3, to evaluate T_m for 47 Tuc, we take as a reference the $\rho_{\text{star}}(r)$ and $\sigma_{\text{star}}(r)$ at its core radius r_c . For 47 Tuc $a_h = 5.7$ AU. In different GC environments one needs to change not only the value of a_h but also those of the $\rho_{\text{star}}(r)$ and $\sigma_{\text{star}}(r)$ profiles. In the following we will generalize our result for all GCs. We also remind the reader that we evolve Eqs. 23 and 25 until the binary reaches $a_{\text{end}} = 0.01$ AU. We make sure the evolution lies within the Newtonian regime at all times until the end of the simulation.

While BBHs interacting with close-by passing stars is inherently a stochastic process, we treat it here in a deterministic manner. The fact that from this point on, we exclude all BBHs with initial conditions (a_0, e_0) that for their given environment do not lead to merger in more than 10 Gyr, leads in a lower/conservative value for their merger rate once averaging over all GCs.

In our calculations of the merger timescale we have used up to here the radial distance of $r = r_c$ as a refer-

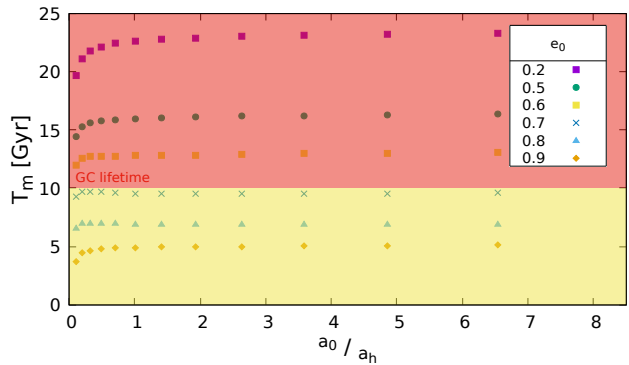


FIG. 3. The 3rd-body merger timescale versus the BBHs initial semimajor axis a_0 . We show cases of $a_0 \in [0.1a_h, 10a_h]$ and plot lines for $e_0 \in [0.2, 0.9]$. Any point that falls inside the yellow region refers to a BBH with initial conditions that in the environment of 47 Tuc will merge at a value of T_m depicted by its y -axis value. We observe a weak dependence on $a_0 \in [a_h, 8a_h]$. For 47 Tuc $a_h = 5.7$ AU at core radius. Each point in this figure is a single simulation.

ence. This choice provides a good description of the 3rd-body interactions inside the GC for a sequence of reasons. For both the King and Plummer profiles, most BHs are included within the core radius. Moreover, for the Plummer profile and for $r \leq r_c$ as we showed in Fig. 1 the total matter density ρ , and the velocity dispersion σ of stellar objects are approximately constant. Thus the 3rd-body interaction terms in Eqs. 23 and 25 that scale as ρ/σ are also constant for $r \lesssim r_c$. Showing the T_m at $r = r_c$ for the Plummer profile is representative of the entire core. For the King profile the ρ/σ drops significantly beyond the $r > r_c$, thus the 3rd-body interactions get suppressed at larger radii. Plotting T_m at $r = r_c$ provides a consecutive but still representative estimate. Finally, we clarify again that in evaluating the total 3rd-body merger rate from Eq. 26 under a general mass profile for the binaries, T_m should be evaluated for different radii r .

While mass segregation also takes place in GCs, forcing stars away from the very center of the clusters the $1 M_\odot$ stars remain within the observed core radii. Given simulation results where BBHs get excited to higher orbits (e.g. [79]), we expect that the $r \sim r_c$ region is still the place where BBHs interact most often with stars.

Our results for the 3rd-body interactions are limited to soft interactions of BBHs with stars. Taking 47 Tuc, the number of hard binaries that survive in the core is expected to be about $\frac{f_{\text{eff}}}{f_{\text{ret}}} \times N_{\text{BH}}^{\text{ret-max}} \simeq 30$ BBHs. This corresponds to a BBH number core density of about 70 pc^{-3} . Also, the BH number core density for 47 Tuc is $\simeq 3000 \text{ pc}^{-3}$. However, the density of stars near its core is $\simeq 10^5 \text{ pc}^{-3}$ or $\simeq 10^6 \text{ pc}^{-3}$, depending on whether we choose the King or the Plummer profile respectively (see Fig. 1). Therefore, BBH-star soft interactions at $r \simeq r_c$ are the most common type with BBH-BH interactions following them (for a recent study of BBH-BH interac-

⁸ When e_0 is smaller than 0.4 for $a_0 = a_h$, initially the binary experiences a slight eccentricity decrease which is due a negative sign in the eccentricity growth rate, supported by numerical surveys [76]. This is a small effect and does not significantly affect the overall growing statistical character of eccentricity with 3rd-body encounters.

GC	$T_{GC} \times 10^{13}$ [yr]	
	Plummer	King
47 Tuc	4.7	0.9
M 30	0.5	0.05
NGC 5946	1.5	0.1

TABLE II. Timescales for a $10 M_{\odot}$ BH to capture and merge with another one at core radius for a few cases. We have assumed the Plummer and King profiles. In all of these cases the numbers exceed the threshold GC lifetime of about 10^{10} yr.

tions see [80]). Binary-binary interactions are rare as the number of BBHs is relatively small in GCs.

B. Binary Black Holes in any GC

1. The Averaged Direct Capture Merger Timescale

In table II we calculate the direct capture timescale for three Milky Way GCs with similar structural properties calculated for BHs at core radius and for the Plummer and King profiles.

Having examined the DC timescale on three dense GCs, we conclude that for those environments this timescale exceeds the GC lifetime by at least one order of magnitude. We find that no known Milky Way GC has a T_{DC} that is smaller than 10 Gyr. This indicates that DC events are very rare in Milky Way GCs. This will show up even in the final merger rates that we calculate in the next section. We expect the DC channel to dominate only in exotic environments with very high densities and with a very low velocity dispersion.

2. The 3rd-body Merger Timescale

In section III A we showed in Figure 3 that a BBH undergoing 3rd-body interactions with stars in 47 Tuc will merge within 10 Gyr only if its initial eccentricity is $e_0 \gtrsim 0.7$; with weak dependence on its initial semi-major axis a_0 . That result came for the specific environment of 47 Tuc. In this section we will generalize our results for any GC. Knowing what initial eccentricity conditions are required in order for a BBH to merge is a crucial element in our calculations. We can simulate the BBH's initial eccentricity distribution in a GC environment, and in turn derive what fraction of those BBHs will merge through the 3rd-body channel.

In the following we will show a sequence of approximations that lead to a semi-analytical answer on the required initial eccentricity conditions for a BBH to merge at any given cluster. That answer we will compare to our answer from the numerical evolution of Eqs. 23 and 25.

Given Eq. 23 we can calculate the time after which the Peters GW emission dominates over the interaction term.

We call this moment in the binary's evolution the equality point. This corresponds to the state (a_{eq}, e_{eq}) . We evaluate the semi-major axis at that point a_{eq} by equating the two rates, $(\dot{a})_{3rd-body} = (\dot{a})_{Peters}$. The e_{eq} could be approximated with $\approx e_{max}$, as the point of equality occurs only slightly after the point of maximum eccentricity e_{max} . However, the condition $\dot{e} = 0$ leads to a transcendental equation for e_{max} which does not have a closed form solution. Thus, instead we set $e_{eq} \simeq e_0$, i.e. at the moment when the binary's eccentricity becomes again e_0 . We checked for the ensemble of clusters at Table I and for initial eccentricities e_0 between 0.4 and 0.9 that the ratio $e_{eq}/e_0 = e_{max}/e_0$ falls always within the region of 1.03 up to 1.30.

The time required for the binary to reach equality $T_{eq}(r)$ if located at radius r , is approximated by integrating Eq. 23 from a_0 to a_{eq} , and ignoring the Peters term which dominates after equality. The result is,

$$T_{eq}(r) = \left(\frac{a_0}{a_{eq}} - 1 \right) \frac{\sigma_{star}(r)}{GH \rho_{star}(r) a_0}. \quad (28)$$

Since in all cases where multiple 3rd-body interactions take place before GW emission starts having an impact to the binary's evolution we can take in Eq. 28 $(a_0/a_{eq} - 1)(1/a_0) \simeq 1/a_{eq}$ ⁹. We then get,

$$T_{eq}(r) \simeq T_m^{s-a}(r) = 5.75 \left(\frac{\sigma_{star}(r)}{10 \text{ km/s}} \right)^{4/5} \left(\frac{15}{H} \right)^{4/5} \times \left(\frac{10^5 M_{\odot}/\text{pc}^3}{\rho_{star}(r)} \right)^{4/5} \left(\frac{10 M_{\odot}}{m_{BH}} \right)^{3/5} \times F^{-1/5}(e_0) \text{ Gyr}. \quad (29)$$

$T_m^{s-a}(r)$ is our semi-analytical evaluation of T_m . To the limit that $a_0 \gg a_{eq}$ satisfied when multiple 3rd-body interactions take place before the binary merges, T_m is independent of a_0 . This is in qualitative agreement with our simulations for 47 Tuc. We also tested the accuracy of Eq. 29 with the numerical results. This is shown in Table III for 47 Tuc, M 30, and NGC 5946. We picked those three clusters as they envelope the $\rho_{star}(r)$ and $\sigma_{star}(r)$ profile properties of the ensemble of clusters that can contribute to the merger. We find these values quite satisfactory for our purposes.

We note that for high eccentricities the semi-analytical answer is larger than the numerical result. At higher eccentricities the GW emission from the Peters term is dominant and Eq. 28 becomes less accurate. Moreover, we use $F(e_0)$ instead of $F(e_{eq})$ in Eq. 29 which at larger eccentricities leads to overestimating T_m^{s-a} . This semi-analytical approach works best at smaller eccentricities, but with satisfactory results for up to $e \approx 0.9$ (see Table III).

⁹ a_{eq} is just evaluated by equating the two terms of the right-hand side of Eq. 23.

GC	e_0	T_m^{num} [Gyr]	$T_m^{\text{S-a}}$ [Gyr]
47 Tuc	0.2	22.6	20.5
47 Tuc	0.8	7.0	8.4
M 30	0.2	7.1	6.9
M 30	0.8	1.2	2.8
NGC 5946	0.2	15.4	14.6
NGC 5946	0.9	2.5	3.7

TABLE III. A few numerical and the corresponding semi-analytical values of T_m as obtained from Eq. 29. We checked 47 Tuc, M 30 and NGC 5946 with two values of e_0 . a_0 is set to the a_h , which is, $a_h = 5.7$ AU for 47 Tuc, $a_h = 47$ AU for M 30, and $a_h = 33$ AU for NGC 5946. Variables are assumed in the context of the King profile at core radius.

The semi-analytical expression of Eq. 29 connects the merger time of the BBH to its initial eccentricity and to the mass density $\rho_{\text{star}}(r)$ and velocity dispersion $\sigma_{\text{star}}(r)$ of the GCs' stars at a radial distance of r . That is, we have a dependence scheme of the form $T_m \propto (\sigma/\rho)^{4/5} F^{-1/5}(e_0)$. We can therefore, set constraints on the minimum initial eccentricity the BBH should have in order for it to merge within the lifetime of the GC, T_{GC} and connect to GC quantities that can be inferred from observations. We remind that we can evaluate ρ_{star} and σ_{star} at the GC's core radius, r_c . I.e. $\sigma_c \equiv \sigma_{\text{star}}(r_c)$ and $\rho_c \equiv \rho_{\text{star}}(r_c)$. We get (see again Eq. 24 for the definition of $F(e)$),

$$F(e_0) > \left(\frac{5.75 \text{ Gyr}}{T_{GC}}\right)^5 \left(\frac{\sigma_c}{10 \text{ km/s}}\right)^4 \left(\frac{10^5 M_\odot/\text{pc}^3}{\rho_c}\right)^4 \times \left(\frac{15}{H}\right)^4 \left(\frac{10 M_\odot}{m_{BH}}\right)^3. \quad (30)$$

Eq. 30 can also be thought of as a constraint on the ratio σ_c/ρ_c given an initial eccentricity e_0 . Therefore, we can probe for an appropriate value of e_0 which environments allow a BBH to merge in T_{GC} given the pair (ρ_c, σ_c) ,

$$\log_{10} \left(\frac{\sigma_c}{10 \text{ km/s}}\right) = \log_{10} \left(\frac{\rho_c}{10^5 M_\odot/\text{pc}^3}\right) + \log_{10} \left(\frac{H}{15}\right) + 0.75 \log_{10} \left(\frac{m_{BH}}{10 M_\odot}\right) + 1.25 \log_{10} \left(\frac{T_{GC}}{5.75 \text{ Gyr}}\right) + 0.25 \log_{10} (F(e_0)). \quad (31)$$

As we can see this condition is fairly insensitive to either the exact age of the GCs and to the exact mass of the BHs.

In Fig. 4 we map out in the observable (ρ_c, σ_c) -parameter space some Milky Way GCs, along with a few specific curves on the required initial eccentricity for binaries of $10 M_\odot$ BHs to merge within 10 Gyr. We take also $H = 15$. These curves correspond to straight lines in a log-log plot. For a given GC its BBHs with initial

eccentricity e_0 larger than the line to its left will merge within 10 Gyr.

As shown in Fig. 4 there are Milky Way GCs, as M 30, that pose no constraints on the initial eccentricity. In these GCs BBHs merge within at most 10 Gyr independent of what their e_0 . This is attributed to their high core densities. However, GCs like M 30 host a small number of BHs and as we will show do not contribute too much on the final merger rates. Instead, in clusters as 47 Tuc, the imposed constraints are only mild. 47 Tuc falls near the $e_0 = 0.7$ line, a result consistent with Figure 3.

In Fig. 5, we show all GC for which we have information to place them on a more extended ρ_c vs σ_c space. With the exception of a few very dense systems, GCs that fall outside the reduced space plotted on Fig. 4 will not contribute significantly to the merger rate even if there are many more of these objects. On general grounds, for environments with $\rho_c \in [0.1, 0.5] \times 10^5 M_\odot/\text{pc}^3$ there is a strong dependence of the minimal e_0 value that leads to a merger and the local velocity dispersion. High velocity environments will host BBH merger only for relatively high e_0 values. In Fig. 4 we take a King profile for the GCs. For a Plummer profile since $\sigma_c^{\text{Plummer}} > \sigma_c^{\text{King}}$ (see Fig. 1) the minimal e_0 values are typically higher. GCs points move to up and to the right. We show that effect in Fig. 4 with green boxes for a small number of GCs. BBHs in GC environments situated on the left of the $e_0 = 0.9$ line should necessarily have an initial eccentricity greater than 0.9 if they are to satisfy Eq. 30. Such binaries are expected to form dynamically and contribute to the dynamical component of the total merger rate.

C. Merger Rates of the Milky Way Globular Clusters

Here we first evaluate the merger rates for individual clusters. We do that separately for the direct capture and for the 3rd-body interactions channel. We rely on Eqs. 15 and 26 respectively. Then we sum the merger rates from all Milky Way globular clusters to evaluate the expected rate from a collection such as that of our own galaxy.

1. DC merger rate

The direct capture merger is a stochastic process. Calculating the DC merger rate from Eq. 15, we show our results in the second and fourth columns of table IV, under the Plummer and King profiles respectively. We use the set of 13 GCs given in table I.

Since the DC merger rate scales as $\Gamma_{DC} \propto n_{BH}^2 \sigma_{BH}^{-11/7}$, the GC with the largest rates will be those that have a small velocity dispersion and large BH densities. Among the cases we have examined, M 30 is one of those dense GCs which also have a small velocity dispersion under the King profile. This GC is a good candidate for a

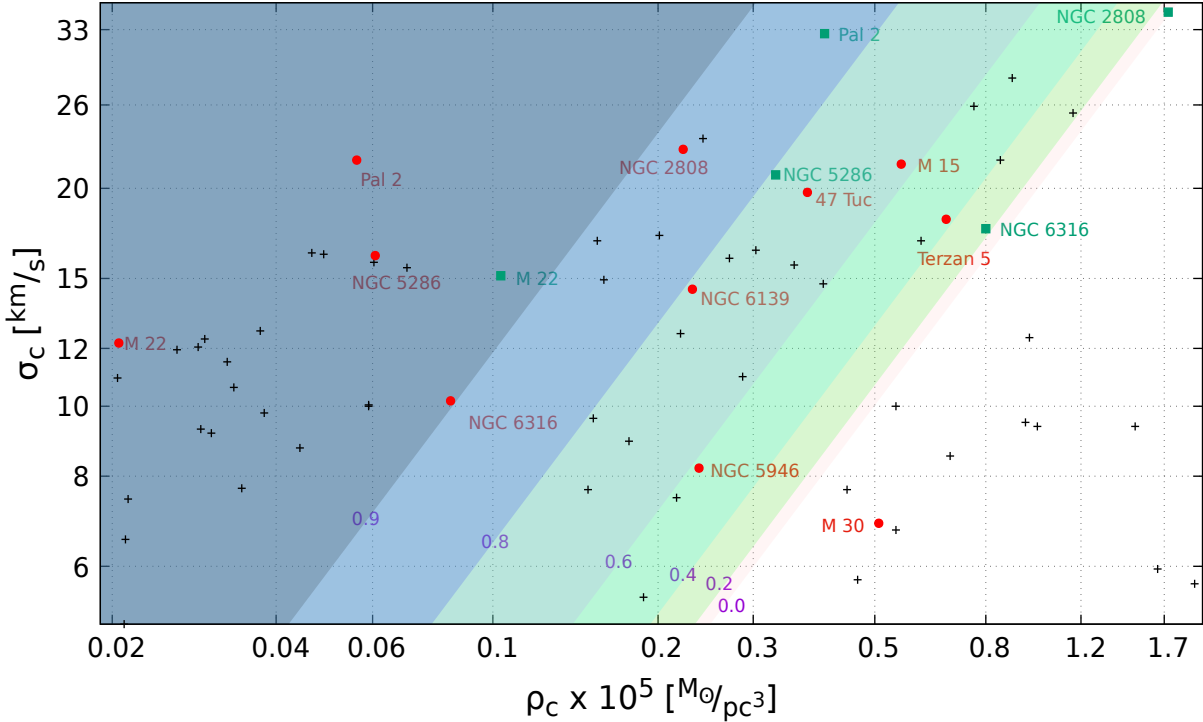


FIG. 4. Milky Way GCs positioned in the ρ_c vs σ_c parameter space for a small part of the observed space (see also Fig. 5). We plot the GCs and partition the selected area into seven regions, with color boundary lines defined by Eq. 31. Labels on the boundary lines represent values of e_0 . For a given GC, its BBHs with e_0 larger than the e_0 -line to its left will merge within 10 Gyr. As an example Terzan 5 sits very close to the line of $e_0 = 0.4$. All its BBHs with e_0 larger than 0.4 will merge. Red dots are GCs from Table I, and green boxes represent GCs under the Plummer profile, while other points are other known GCs.

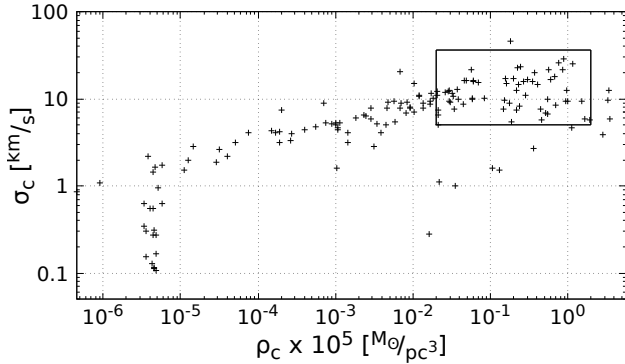


FIG. 5. All observed Milky Way GCs in the full ρ_c vs σ_c parameter space. The box on the top left represents the parameter space of the Fig. 4. The black "+" points represent GCs under the King profile.

high DC merger rate, as we also saw in table II where the DC timescale was calculated to be relatively small compared to other GCs. The King DC rate of M 30 is about $2.1 \times 10^{-10} \text{yr}^{-1}$ and is among the highest on the list.

We perform an average on the DC merger rate over the known 139 Milky Way GCs of the Harris catalogue

[57, 62], that we have ρ and σ information for. We find an averaged DC rate of $4.9 \times 10^{-11} \text{yr}^{-1}$ per cluster relying on the King profile. Using the Plummer profile for the stars we find instead a per cluster rate of $3.3 \times 10^{-12} \text{yr}^{-1}$. Typically and on average the King DC rate is higher than the Plummer one by about an order of magnitude. This can be seen by comparing for the individual GC the DC rates in Table IV. The King profile typically predicts a lower velocity dispersion compared to the Plummer model around the core radius of each GC, (see Fig. 1).

2. 3rd-body merger rate

For the 3rd-body interactions as we showed, the initial eccentricity of a BBH hosted on a GC plays a crucial role on whether that binary will have enough time to merge. To calculate the merger rate we assume a thermal distribution of the BBH's eccentricity, $P(e) = 2 \cdot e$, with a mean of $\langle e \rangle = 0.7$. We then evaluate for each Milky Way GC the f_e of Eq. 26 from,

$$f_e(r) \equiv \int_{e_0(r)}^1 de'_0 P(e'_0) = 1 - e_0(r)^2. \quad (32)$$

e_0 is the minimal initial eccentricity required for a BBH to merge within 10 Gyr, calculated for each GC by equating the two sides of Eq. 30 with $T_{GC} = 10$ Gyr and using the unique GC's σ_c and ρ_c properties. A thermal distribution is consistent with a dynamical assembly scenario of our BBHs, [67]. Proto-binaries may acquire high initial eccentricities by the internal dynamics during the formation of the BBH pair. We concentrate on hard BBHs. We take for them $a_0 = a_h$, with a_h having a unique value for each mass profile (and each GC). Binaries hosted in an environment described by a Plummer mass profile, begin tighter (a_h is smaller) compared to a same mass cluster with a King mass profile. The smaller a_h is a consequence of the larger velocity dispersion of these objects in a Plummer profile, (see Fig. 1). However, our results are fairly insensitive to the exact choice of a_0 (see Fig. 3 and Eq. 29). Initial semi-major axes smaller than $\sim 0.3a_h$ have a smaller merger time than we consider in this work. Yet, these ultra-hard binaries are rare.

GC	Plummer		King	
	DC	3rd-body	DC	3rd-body
47 Tuc	1.2e-11	3.4e-09	7.6e-11	1.5e-09
ω Cen	1.8e-13	9.8e-11	3.5e-13	2.2e-11
M 15	3.0e-11	6.2e-09	3.1e-10	3.7e-09
M 22	1.8e-13	9.9e-11	3.4e-13	2.1e-11
NGC 6362	4.3e-15	9.0e-13	3.5e-15	2.7e-13
NGC 5946	8.8e-12	8.5e-10	1.9e-10	5.6e-10
M 30	9.8e-12	3.4e-10	2.1e-10	3.4e-10
Terzan 5	3.7e-12	6.8e-10	9.4e-12	5.5e-10
Pal 2	1.1e-12	9.5e-10	3.2e-12	1.7e-10
NGC 6139	3.2e-12	1.1e-09	1.2e-11	3.9e-10
NGC 2808	2.5e-12	2.0e-09	7.2e-12	4.5e-10
NGC 5286	5.1e-13	3.5e-10	1.1e-12	7.5e-11
NGC 6316	6.1e-13	3.5e-10	1.2e-12	6.8e-11

TABLE IV. The integrated DC and 3rd-body merger rates, in yr^{-1} , for our 13 Milky Way GCs. The parameter f_{eff} is set to 0.3%.

The 3rd-body merger rates for the GCs of Table I are given in Table IV, for the two choices of mass profiles. The 3rd-body merger rate surpasses the DC rate by typically one to two orders of magnitude. This is despite the fact that BBHs are less abundant by a factor of 3×10^2 than isolated BHs that seed the DC events. 47 Tuc falls in the category of a massive GC and NGC 6362 represents a small GC.

Following the King profile we get typically a factor of two smaller rates, even though in some cases as M 30 the rate is the same for both assumed profiles on the distribution of the stars. We find that the average per cluster rate of the 3rd-body channel is $2.0 \times 10^{-10} \text{yr}^{-1}$ under the King profile assumptions for the stars and $4.2 \times 10^{-10} \text{yr}^{-1}$ per cluster under the Plummer.

In the numbers of Table IV we have taken $f_{\text{eff}} = 0.3\%$. f_{eff} is in the range of $0.1\% \leq f_{\text{eff}} \leq 1\%$ which directly translates to one order of magnitude in range of the 3rd-body merger rate. That uncertainty is the main source of uncertainty on evaluating the 3rd-body merger rate from

a given GC.

We make a last note here regarding the ejection of binaries from the globular clusters. During each encounter of a BBH with a perturbing object (a star in our case), the perturbing object acquires on average a high kick and by momentum conservation the binary recoils. We have checked that in order for the BBH to receive a large enough recoil to get ejected from the GC environment the interaction has to be very close and in turn the binary already at that stage a tight one. BBHs encountering $1 M_\odot$ stars tend to be retained near the GC core as long as they have a semi-major axis of $\gtrsim 0.01$ AU before the interaction. We remind the reader that for our 3rd-body calculations we use that value of semi-major axis to end our evolution of the binaries' orbital properties. Once the binary has a semi-major axis smaller than 0.01 AU it only takes a few Myr until it merges via GW emission. Regardless of such a binary still being in the cluster or having been ejected from it, its merger contributes to our calculation of the merger rate.

D. The Cosmological Merger Rate

Having evaluated the merger rate in the GCs of the Milky Way and the averaged per cluster merger rate $\langle \Gamma_{GC} \rangle$ we will evaluate the cumulative merger rate at redshift z from the local Universe, $\mathcal{R}_c(z)$. Formally $\langle \Gamma_{GC} \rangle$ is a function of redshift. However, we will take it a constant over a period of 10 Gyrs and will not extend our analysis beyond a redshift of 5. This can be calculated by [32, 81],

$$\mathcal{R}_c(z) = \int_0^z dz' \langle \Gamma_{GC}(z') \rangle n_{GC} \frac{dV_c}{dz'} (1+z')^{-1}. \quad (33)$$

where dV_c/dz is the comoving volume, $n_{GC}(z)$ is the GC number density and the $(1+z)^{-1}$ factor accounts for the time dilation. $\langle \Gamma_{GC} \rangle$, for the combination of the DC and the 3rd-body channels, we have already estimated to be $2.5 \times 10^{-10} \text{yr}^{-1}$ and $4.2 \times 10^{-10} \text{yr}^{-1}$ per cluster for the King and Plummer profiles respectively. At low redshift n_{GC} has a range from a conservative minimum of $0.33 \times 10^9 \text{Gpc}^{-3}$ up to an optimistic value of $\simeq 3 \times 10^9 \text{Gpc}^{-3}$, with a more conventional value of $0.77 \times 10^9 \text{Gpc}^{-3}$ [32]. We assume that Milky Way GCs constitute a representative ensemble of GCs in the local Universe. In the following, we take $H_0 = 100h \text{ km/s/Mpc}$, $h = 0.7$, $\Omega_K = 0$, $\Omega_M = 0.3$ and $\Omega_\Lambda = 0.7$, based on Planck data (2015) [82]. We can rewrite the comoving volume as, [83],

$$\frac{dV_c}{dz'} = \frac{4\pi c^3}{H_0^3} \frac{1}{E(z')} \left(\int_0^{z'} \frac{dz''}{E(z'')} \right)^2, \quad (34)$$

where we have used the function, [83, 84],

$$E(z) = \sqrt{\Omega_M \cdot (1+z)^3 + \Omega_\Lambda}. \quad (35)$$

We take the more conventional value of $n_{GC} = 0.77 \times 10^9 \text{Gpc}^{-3}$ constant in redshift or evolving as $n_{GC}(z) =$

$0.77 \times 10^9 \cdot E(z) \text{ Gpc}^{-3}$. Integrating up to a redshift of 1, we find a rate of 20-65 mergers per year for the choice of a King profile and 33-110 mergers for the choice of a Plummer profile. For each of the profiles the higher values for the mergers come from assuming $n_{GC} \propto E(z)$. Extending to higher redshifts comes with a significant increase associated to the uncertainties on the exact choice of $n_{GC}(z)$. The total number of BBHs mergers up redshift of 5 can be as large as 10^4 mergers per year for the King and Plummer profiles respectively. However for a nearly constant in redshift n_{GC} these numbers are much more suppressed and only $O(100)$ per year.

We note that the DC merger rate per GC at source is taken to be constant with redshift up to $z = 5$ while for the 3rd-body merger rate its redshift evolution is described by the term $\langle f_e(r) \rangle / T_{GC}$ of Eq. 26 through the lifetime of the GC evaluated at redshift z' .

IV. CONCLUSIONS

In this paper we evaluate the BH-BH merger rates in Milky Way type GCs considering BH-BH direct capture and 3rd-body BBH-star soft interaction mechanisms. Our calculations are based under the assumption of a two-mass model of $m_{\text{star}} = 1 M_{\odot}$ and $m_{BH} = 10 M_{\odot}$. We consider King and Plummer profiles for the distribution of the stars in the GCs, and take a segregated state on the BHs concentrating all of them uniformly inside the core of each GC.

The averaged 3rd-body merger rate per cluster was found to be $2.0 \times 10^{-10} \text{ yr}^{-1}$ and $4.2 \times 10^{-10} \text{ yr}^{-1}$ for the King and Plummer profiles. These rates are more significant than the rates from the DC channel by one to two orders of magnitude. For the DC channel we get instead $4.9 \times 10^{-11} \text{ yr}^{-1}$ and $3.3 \times 10^{-12} \text{ yr}^{-1}$ for the King and Plummer profiles respectively.

The largest uncertainty with respect to the BBH merger rates is in the fraction f_{eff} of BBHs that can be formed from the original population of BHs created by stellar evolution, and then undergo multiple 3rd-body interactions with stars. Most BHs will be ejected from the clusters due to their natal kicks. Also most BHs that remain in the cluster will not be in binaries that are tight enough to survive the 3rd-body interactions even with regular stars. Throughout this work we take $f_{eff} = 0.3\%$. That fraction's range is between 0.1% to 1%. Our re-

sults on the merger rates from the 3rd-body channel are proportional to $(f_{eff}/0.3\%)$.

Once integrating over cosmological distances we find in total between 20 and 110 mergers per year up to a redshift of $z = 1$. We note that in calculating the cumulative rates, the numbers are dominated by the most dense and massive clusters. These clusters are also the easiest to observe. Clusters with small core densities or masses maybe difficult to observe but also do not contribute to the our rates in any significant manner.

In this work we have quantified an important aspect of the 3rd-body channel in GCs. The initial eccentricity of the BBH plays a crucial role in the evolution of the binary given its surroundings and whether it will evolve fast enough to merge within a Hubble time. Only very compact GCs allow the presence of low eccentricity mergers. As an example, an environment like 47 Tuc requires BBHs to have an eccentricity of no less than ~ 0.7 which is the average value of the thermal eccentricity distribution. Instead, the BBH's merger time depends weakly on the initial semi-major axis.

Our results are limited to soft interactions of BBHs with stars, as these are the most common type of interactions. As this project was being completed Ref. [80] appeared studying BBH-BH hard interactions. Other possible channels leading to BBH merges that we have not included in this work as they are not dominant, relate to four body effects. One such mechanism is the Kozai resonance, [85, 86], as known in the literature in the context of triple systems (hierarchical or not) [54–56]. This channel requires a triple system where two of the objects are BHs forming an inner compact binary and a third object, a BH or a star, that orbits in an outer orbit. The outer object, causes the eccentricity of the inner pair to increase near unity on a timescale of a few hundred years, on condition that the two orbits have a relative inclination close to 90 degrees and that no other object perturbs the system in the meantime [87]. The two inner BHs can merge very quickly if the GW emission peaks near the phase of high eccentricity. The contribution from this channel to the BBH merger rate is highly suppressed, due to the small number of BBHs inside of GCs. The statistics of such a mechanism work best inside of denser and larger environments like the cores of galaxies where the number of BHs and BBHs are higher.

Acknowledgements: The authors are grateful to A. Kehagias for his support in facilitating this collaboration.

[1] J. Aasi *et al.* (LIGO Scientific), “Advanced LIGO,” *Class. Quant. Grav.* **32**, 074001 (2015), arXiv:1411.4547 [gr-qc].
 [2] B.P. Abbott *et al.* (LIGO Scientific, Virgo), “Binary Black Hole Population Properties Inferred from the First and Second Observing Runs of Advanced LIGO and Advanced Virgo,” *Astrophys. J. Lett.* **882**, L24 (2019), arXiv:1811.12940 [astro-ph.HE].
 [3] Hans A. Bethe and G.E. Brown, “Evolution of binary

compact objects which merge,” *Astrophys. J.* **506**, 780–789 (1998), arXiv:astro-ph/9802084.
 [4] Simon F. Portegies Zwart and Stephen McMillan, “Black hole mergers in the universe,” *Astrophys. J. Lett.* **528**, L17 (2000), arXiv:astro-ph/9910061.
 [5] Krzysztof Belczynski, Vassiliki Kalogera, and Tomasz Bulik, “A Comprehensive study of binary compact objects as gravitational wave sources: Evolutionary chan-

- nels, rates, and physical properties,” *Astrophys. J.* **572**, 407–431 (2001), arXiv:astro-ph/0111452.
- [6] Ryan M. O’Leary, Bence Kocsis, and Abraham Loeb, “Gravitational waves from scattering of stellar-mass black holes in galactic nuclei,” *Mon. Not. Roy. Astron. Soc.* **395**, 2127–2146 (2009), arXiv:0807.2638 [astro-ph].
- [7] Sambaran Banerjee, Holger Baumgardt, and Pavel Kroupa, “Stellar-mass black holes in star clusters: implications for gravitational wave radiation,” *Mon. Not. R. Astron. Soc.* **402**, 371–380 (2010), arXiv:0910.3954 [astro-ph.SR].
- [8] Fabio Antonini and Hagai B. Perets, “Secular evolution of compact binaries near massive black holes: Gravitational wave sources and other exotica,” *Astrophys. J.* **757**, 27 (2012), arXiv:1203.2938 [astro-ph.GA].
- [9] B. McKernan, K. E. S. Ford, W. Lyra, and H. B. Perets, “Intermediate mass black holes in AGN discs - I. Production and growth,” *Mon. Not. R. Astron. Soc.* **425**, 460–469 (2012), arXiv:1206.2309 [astro-ph.GA].
- [10] Michal Dominik, Krzysztof Belczynski, Christopher Fryer, Daniel E. Holz, Emanuele Berti, Tomasz Bulik, Ilya Mandel, and Richard O’Shaughnessy, “Double Compact Objects II: Cosmological Merger Rates,” *Astrophys. J.* **779**, 72 (2013), arXiv:1308.1546 [astro-ph.HE].
- [11] M. Mapelli, L. Zampieri, E. Ripamonti, and A. Bressan, “Dynamics of stellar black holes in young star clusters with different metallicities - I. Implications for X-ray binaries,” *Mon. Not. R. Astron. Soc.* **429**, 2298–2314 (2013), arXiv:1211.6441 [astro-ph.HE].
- [12] Brunetto Marco Ziosi, Michela Mapelli, Marica Branchesi, and Giuseppe Tormen, “Dynamics of stellar black holes in young star clusters with different metallicities - II. Black hole–black hole binaries,” *Mon. Not. Roy. Astron. Soc.* **441**, 3703–3717 (2014), arXiv:1404.7147 [astro-ph.GA].
- [13] Fabio Antonini and Frederic A. Rasio, “Merging black hole binaries in galactic nuclei: implications for advanced-LIGO detections,” *Astrophys. J.* **831**, 187 (2016), arXiv:1606.04889 [astro-ph.HE].
- [14] Simeon Bird, Ilias Cholis, Julian B. Muñoz, Yacine Ali-Haïmoud, Marc Kamionkowski, Ely D. Kovetz, Alvise Raccanelli, and Adam G. Riess, “Did LIGO detect dark matter?” *Phys. Rev. Lett.* **116**, 201301 (2016), arXiv:1603.00464 [astro-ph.CO].
- [15] Misao Sasaki, Teruaki Suyama, Takahiro Tanaka, and Shuichiro Yokoyama, “Primordial Black Hole Scenario for the Gravitational-Wave Event GW150914,” *Phys. Rev. Lett.* **117**, 061101 (2016), [Erratum: *Phys.Rev.Lett.* **121**, 059901 (2018)], arXiv:1603.08338 [astro-ph.CO].
- [16] Nicholas C. Stone, Brian D. Metzger, and Zoltán Haiman, “Assisted inspirals of stellar mass black holes embedded in AGN discs: solving the ‘final au problem’,” *Mon. Not. Roy. Astron. Soc.* **464**, 946–954 (2017), arXiv:1602.04226 [astro-ph.GA].
- [17] Bernard Carr, Florian Kuhnel, and Marit Sandstad, “Primordial Black Holes as Dark Matter,” *Phys. Rev. D* **94**, 083504 (2016), arXiv:1607.06077 [astro-ph.CO].
- [18] Abbas Askar, Magdalena Szkudlarek, Dorota Gondok-Rosińska, Mirek Giersz, and Tomasz Bulik, “MOCCA-SURVEY Database - I. Coalescing binary black holes originating from globular clusters,” *Mon. Not. Roy. Astron. Soc.* **464**, L36–L40 (2017), arXiv:1608.02520 [astro-ph.HE].
- [19] Simon Stevenson, Alejandro Vigna-Gómez, Ilya Mandel, Jim W. Barrett, Coenraad J. Neijssel, David Perkins, and Selma E. de Mink, “Formation of the first three gravitational-wave observations through isolated binary evolution,” *Nature Commun.* **8**, 14906 (2017), arXiv:1704.01352 [astro-ph.HE].
- [20] Mario Spera, Michela Mapelli, Nicola Giacobbo, Alessandro Alberto Trani, Alessandro Bressan, and Guglielmo Costa, “Merging black hole binaries with the SEVN code,” (2018), 10.1093/mnras/stz359, arXiv:1809.04605 [astro-ph.HE].
- [21] Michela Mapelli and Nicola Giacobbo, “The cosmic merger rate of neutron stars and black holes,” *Mon. Not. Roy. Astron. Soc.* **479**, 4391–4398 (2018), arXiv:1806.04866 [astro-ph.HE].
- [22] Davide Gerosa and Emanuele Berti, “Escape speed of stellar clusters from multiple-generation black-hole mergers in the upper mass gap,” *Phys. Rev. D* **100**, 041301 (2019), arXiv:1906.05295 [astro-ph.HE].
- [23] Vishal Baibhav, Davide Gerosa, Emanuele Berti, Kaze W.K. Wong, Thomas Helfer, and Matthew Mould, “The mass gap, the spin gap, and the origin of merging binary black holes,” (2020), arXiv:2004.00650 [astro-ph.HE].
- [24] Ely D. Kovetz, Ilias Cholis, Patrick C. Breysse, and Marc Kamionkowski, “Black hole mass function from gravitational wave measurements,” *Phys. Rev. D* **95**, 103010 (2017), arXiv:1611.01157 [astro-ph.CO].
- [25] J. J. Eldridge, E. R. Stanway, L. Xiao, L. A. S. McClelland, G. Taylor, M. Ng, S. M. L. Greis, and J. C. Bray, “Binary population and spectral synthesis version 2.1: Construction, observational verification, and new results,” *Publications of the Astronomical Society of Australia* **34** (2017), 10.1017/pasa.2017.51.
- [26] Ilya Mandel, Will M. Farr, and Jonathan R. Gair, “Extracting distribution parameters from multiple uncertain observations with selection biases,” *Mon. Not. Roy. Astron. Soc.* **486**, 1086–1093 (2019), arXiv:1809.02063 [physics.data-an].
- [27] Yann Bouffanais, Michela Mapelli, Davide Gerosa, Ugo N. Di Carlo, Nicola Giacobbo, Emanuele Berti, and Vishal Baibhav, “Constraining the fraction of binary black holes formed in isolation and young star clusters with gravitational-wave data,” *Astrophys. J.* **886** (2019), 10.3847/1538-4357/ab4a79, arXiv:1905.11054 [astro-ph.HE].
- [28] Vishal Baibhav, Emanuele Berti, Davide Gerosa, Michela Mapelli, Nicola Giacobbo, Yann Bouffanais, and Ugo N. Di Carlo, “Gravitational-wave detection rates for compact binaries formed in isolation: LIGO/Virgo O3 and beyond,” *Phys. Rev. D* **100**, 064060 (2019), arXiv:1906.04197 [gr-qc].
- [29] Ryan M. O’Leary, Frederic A. Rasio, John M. Fregeau, Natalia Ivanova, and Richard W. O’Shaughnessy, “Binary mergers and growth of black holes in dense star clusters,” *Astrophys. J.* **637**, 937–951 (2006), arXiv:astro-ph/0508224.
- [30] J. M. B. Downing, M. J. Benacquista, M. Giersz, and R. Spurzem, “Compact binaries in star clusters - I. Black hole binaries inside globular clusters,” *Mon. Not. R. Astron. Soc.* **407**, 1946–1962 (2010), arXiv:0910.0546 [astro-ph.SR].
- [31] Carl L. Rodriguez, Meagan Morscher, Bharath Pattabiraman, Sourav Chatterjee, Carl-Johan Haster, and Frederic A. Rasio, “Binary Black Hole Mergers from Globular

- Clusters: Implications for Advanced LIGO,” *Phys. Rev. Lett.* **115**, 051101 (2015), [Erratum: *Phys. Rev. Lett.* **116**, 029901 (2016)], arXiv:1505.00792 [astro-ph.HE].
- [32] Carl L. Rodriguez, Sourav Chatterjee, and Frederic A. Rasio, “Binary Black Hole Mergers from Globular Clusters: Masses, Merger Rates, and the Impact of Stellar Evolution,” *Phys. Rev. D* **93**, 084029 (2016), arXiv:1602.02444 [astro-ph.HE].
- [33] Giacomo Fragione and Bence Kocsis, “Black hole mergers from an evolving population of globular clusters,” *Phys. Rev. Lett.* **121**, 161103 (2018), arXiv:1806.02351 [astro-ph.GA].
- [34] Jongsuk Hong, Enrico Vesperini, Abbas Askar, Mirek Giersz, Magdalena Szkudlarek, and Tomasz Bulik, “Binary black hole mergers from globular clusters: the impact of globular cluster properties,” *Monthly Notices of the Royal Astronomical Society* **480**, 5645–5656 (2018).
- [35] Carl-Johan Haster, Fabio Antonini, Vicky Kalogera, and Ilya Mandel, “N-body dynamics of intermediate mass-ratio inspirals in star clusters,” *The Astrophysical Journal* **832**, 192 (2016).
- [36] Dawoo Park, Chunglee Kim, Hyung Mok Lee, Yeong-Bok Bae, and Krzysztof Belczynski, “Black hole binaries dynamically formed in globular clusters,” *Monthly Notices of the Royal Astronomical Society* **469**, 4665–4674 (2017).
- [37] Václav Pavlík, Tereza Jeřábková, Pavel Kroupa, and Holger Baumgardt, “The black hole retention fraction in star clusters,” *Astronomy & Astrophysics* **617**, A69 (2018).
- [38] Maya Fishbach, Daniel E. Holz, and Ben Farr, “Are LIGO’s Black Holes Made From Smaller Black Holes?” *Astrophys. J. Lett.* **840**, L24 (2017), arXiv:1703.06869 [astro-ph.HE].
- [39] Ely D. Kovetz, Ilias Cholis, Marc Kamionkowski, and Joseph Silk, “Limits on Runaway Growth of Intermediate Mass Black Holes from Advanced LIGO,” *Phys. Rev. D* **97**, 123003 (2018), arXiv:1803.00568 [astro-ph.HE].
- [40] Fabio Antonini, Mark Gieles, and Alessia Gualandris, “Black hole growth through hierarchical black hole mergers in dense star clusters: implications for gravitational wave detections,” *Mon. Not. Roy. Astron. Soc.* **486**, 5008–5021 (2019), arXiv:1811.03640 [astro-ph.HE].
- [41] Maya Fishbach and Daniel E. Holz, “Where Are LIGO’s Big Black Holes?” *Astrophys. J. Lett.* **851**, L25 (2017), arXiv:1709.08584 [astro-ph.HE].
- [42] Maya Fishbach and Daniel E. Holz, “Picky Partners: The Pairing of Component Masses in Binary Black Hole Mergers,” *Astrophys. J. Lett.* **891**, L27 (2020), arXiv:1905.12669 [astro-ph.HE].
- [43] Davide Gerosa, Salvatore Vitale, and Emanuele Berti, “Astrophysical implications of GW190412 as a remnant of a previous black-hole merger,” (2020), arXiv:2005.04243 [astro-ph.HE].
- [44] Chase Kimball, Colm Talbot, Christopher P.L. Berry, Matthew Carney, Michael Zevin, Eric Thrane, and Vicky Kalogera, “Black hole genealogy: Identifying hierarchical mergers with gravitational waves,” (2020), arXiv:2005.00023 [astro-ph.HE].
- [45] Carl L. Rodriguez *et al.*, “GW190412 as a Third-Generation Black Hole Merger from a Super Star Cluster,” (2020), arXiv:2005.04239 [astro-ph.HE].
- [46] P. C. Peters, “Gravitational Radiation and the Motion of Two Point Masses,” *Physical Review* **136**, 1224–1232 (1964).
- [47] Ilya Mandel, Duncan A. Brown, Jonathan R. Gair, and M. Coleman Miller, “Rates and characteristics of intermediate mass ratio inspirals detectable by advanced ligo,” *The Astrophysical Journal* **681**, 1431–1447 (2008).
- [48] Gerald D. Quinlan and Stuart L. Shapiro, “Dynamical Evolution of Dense Clusters of Compact Stars,” *Astrophys. J.* **343**, 725 (1989).
- [49] Hideaki Mouri and Yoshiaki Taniguchi, “Runaway merging of black holes: analytical constraint on the time scale,” *Astrophys. J. Lett.* **566**, L17–L20 (2002), arXiv:astro-ph/0201102.
- [50] J. G. Hills, “The effect of low-velocity, low-mass intruders (collisionless gas) on the dynamical evolution of a binary system,” *Astron. J.* **88**, 1269–1283 (1983).
- [51] Alberto Sesana, Francesco Haardt, and Piero Madau, “Interaction of massive black hole binaries with their stellar environment. 1. Ejection of hypervelocity stars,” *Astrophys. J.* **651**, 392–400 (2006), arXiv:astro-ph/0604299.
- [52] Carl L. Rodriguez, Pau Amaro-Seoane, Sourav Chatterjee, Kyle Kremer, Frederic A. Rasio, Johan Samsing, Claire S. Ye, and Michael Zevin, “Post-newtonian dynamics in dense star clusters: Formation, masses, and merger rates of highly-eccentric black hole binaries,” *Physical Review D* **98** (2018), 10.1103/physrevd.98.123005.
- [53] Johan Samsing, “Eccentric black hole mergers forming in globular clusters,” *Physical Review D* **97** (2018), 10.1103/physrevd.97.103014.
- [54] M. Coleman Miller and Douglas P. Hamilton, “Four-body effects in globular cluster black hole coalescence,” *The Astrophysical Journal* **576**, 894–898 (2002).
- [55] Manuel Arca-Sedda, Gongjie Li, and Bence Kocsis, “Ordering the chaos: stellar black hole mergers from non-hierarchical triples,” arXiv e-prints, arXiv:1805.06458 (2018), arXiv:1805.06458 [astro-ph.HE].
- [56] Joseph M. O. Antognini and Todd A. Thompson, “Dynamical formation and scattering of hierarchical triples: cross-sections, kozai–lidov oscillations, and collisions,” *Monthly Notices of the Royal Astronomical Society* **456**, 4219–4246 (2016).
- [57] GLOBCLUST Milky Way Globular Clusters Catalog, “<https://heasarc.gsfc.nasa.gov/w3browse/all/globclust.html>,” .
- [58] Ivan King, “The structure of star clusters. I. an empirical density law,” *Astron. J.* **67**, 471 (1962).
- [59] II Collins, G. W., *The virial theorem in stellar astrophysics* (1978).
- [60] H. C. Plummer, “On the problem of distribution in globular star clusters,” *Mon. Not. R. Astron. Soc.* **71**, 460–470 (1911).
- [61] Herwig Dejonghe, “A completely analytical family of anisotropic Plummer models,” *Mon. Not. R. Astron. Soc.* **224**, 13–39 (1987).
- [62] William E. Harris, “A Catalog of Parameters for Globular Clusters in the Milky Way,” *Astron. J.* **112**, 1487 (1996).
- [63] P. Kroupa, “The initial mass function of stars: Evidence for uniformity in variable systems,” *Science* **295**, 82–91 (2002).
- [64] Matthias U. Kruckow, Thomas M. Tauris, Norbert Langer, Michael Kramer, and Robert G. Izzard, “Progenitors of gravitational wave mergers: Binary evolution with the stellar grid-based code ComBinE,”

- Mon. Not. Roy. Astron. Soc. **481**, 1908–1949 (2018), arXiv:1801.05433 [astro-ph.SR].
- [65] Nicola Giacobbo and Michela Mapelli, “The progenitors of compact-object binaries: impact of metallicity, common envelope and natal kicks,” *Mon. Not. Roy. Astron. Soc.* **480**, 2011–2030 (2018), arXiv:1806.00001 [astro-ph.HE].
- [66] Jr. Spitzer, Lyman, “Equipartition and the Formation of Compact Nuclei in Spherical Stellar Systems,” *Astrophys. J. Lett.* **158**, L139 (1969).
- [67] D. C. Heggie, “Binary evolution in stellar dynamics,” *Mon. Not. R. Astron. Soc.* **173**, 729–787 (1975).
- [68] Natalia Ivanova, Vicky Kologera, and Marc van der Sluys, “Evolution of binaries in dense stellar systems,” (2010), 10.1063/1.3536357.
- [69] N. Ivanova, K. Belczynski, J. M. Fregeau, and F. A. Rasio, “The evolution of binary fractions in globular clusters,” *Monthly Notices of the Royal Astronomical Society* **358**, 572–584 (2005).
- [70] J. G. Hills and L. W. Fullerton, “Computer simulations of close encounters between single stars and hard binaries,” *Astron. J.* **85**, 1281–1291 (1980).
- [71] Hideaki Mouri and Yoshiaki Taniguchi, “Runaway merging of black holes: Analytical constraint on the timescale,” *The Astrophysical Journal* **566**, L17–L20 (2002).
- [72] M. Turner, “Gravitational radiation from point-masses in unbound orbits: Newtonian results,” *Astrophys. J.* **216**, 610–619 (1977).
- [73] Ilias Cholis, Ely D. Kovetz, Yacine Ali-Haïmoud, Simeon Bird, Marc Kamionkowski, Julian B. Muñoz, and Alvise Raccanelli, “Orbital eccentricities in primordial black hole binaries,” *Physical Review D* **94** (2016), 10.1103/physrevd.94.084013.
- [74] Ryan M. O’Leary, Bence Kocsis, and Abraham Loeb, “Gravitational waves from scattering of stellar-mass black holes in galactic nuclei,” *Monthly Notices of the Royal Astronomical Society* **395**, 2127–2146 (2009).
- [75] Gerald D. Quinlan, “The dynamical evolution of massive black hole binaries i. hardening in a fixed stellar background,” *New Astronomy* **1**, 35–56 (1996).
- [76] Alberto Sesana, Francesco Haardt, and Piero Madau, “Interaction of massive black hole binaries with their stellar environment. i. ejection of hypervelocity stars,” *The Astrophysical Journal* **651**, 392–400 (2006).
- [77] Steinn Sigurdsson and E. S. Phinney, “Binary–Single Star Interactions in Globular Clusters,” *Astrophys. J.* **415**, 631 (1993).
- [78] Nadia Biava, Monica Colpi, Pedro R. Capelo, Matteo Bonetti, Marta Volonteri, Tomas Tamfal, Lucio Mayer, and Alberto Sesana, “The lifetime of binary black holes in sérsic galaxy models,” *Monthly Notices of the Royal Astronomical Society* **487**, 4985–4994 (2019).
- [79] Johan Samsing, Daniel J. D’Orazio, Kyle Kremer, Carl L. Rodriguez, and Abbas Askar, “Gravitational-wave captures of single black holes in globular clusters,” (2019), arXiv:1907.11231 [astro-ph.HE].
- [80] Johan Samsing and Kenta Hotokezaka, “Populating the Black Hole Mass Gaps In Stellar Clusters: General Relations and Upper Limits,” (2020), arXiv:2006.09744 [astro-ph.HE].
- [81] Claire S. Ye, Wen-fai Fong, Kyle Kremer, Carl L. Rodriguez, Sourav Chatterjee, Giacomo Fragione, and Frederic A. Rasio, “On the Rate of Neutron Star Binary Mergers from Globular Clusters,” *Astrophys. J. Lett.* **888**, L10 (2020), arXiv:1910.10740 [astro-ph.HE].
- [82] P.A.R. Ade *et al.* (Planck), “Planck 2015 results. XIII. Cosmological parameters,” *Astron. Astrophys.* **594**, A13 (2016), arXiv:1502.01589 [astro-ph.CO].
- [83] David W. Hogg, “Distance measures in cosmology,” (1999), arXiv:astro-ph/9905116.
- [84] Yue-Yao Xu and Xin Zhang, “Comparison of dark energy models after Planck 2015,” *Eur. Phys. J. C* **76**, 588 (2016), arXiv:1607.06262 [astro-ph.CO].
- [85] Yoshihide Kozai, “Secular perturbations of asteroids with high inclination and eccentricity,” *Astron. J.* **67**, 591–598 (1962).
- [86] M. L. Lidov, “The evolution of orbits of artificial satellites of planets under the action of gravitational perturbations of external bodies,” *Planetary and Space Science* **9**, 719–759 (1962).
- [87] Smadar Naoz, “The eccentric kozai-lidov effect and its applications,” *Annual Review of Astronomy and Astrophysics* **54**, 441–489 (2016).

Appendix A: Numerical setup for the BBH evolution in the 3rd-body channel

In this appendix we present the numerical setup of our calculations for the case of the evolution of a BBH due to GW emission and interactions with 3rd-bodies.

In Eqs. 23 and 25 the term describing the 3rd-body interactions with stars has a proportionality coefficient K . That coefficient is not constant but depends on the value of the binary’s eccentricity and semi-major axis. We rely on the numerical work by [51] to include that dependence. In Fig. 6 we show the fitting functions we use for the evolution of a BBH as were provided in [51]. We implement a cubic fit on the data in their table 3. These fits are accurate only for values of eccentricity on the interval $e \in [0.15, 0.9]$.

An important parameter we should set in our simulations is the time-step, dt . The first term in the right hand side of Eq. 23 sets an upper limit on the time-step we should use, since it relies on Eq. 20 which describes a single interaction. Our time-step has to be bigger than the period of the binary so that the Peters term remains secular. This sets a lower bound. We can choose our the numerical time-step to be that of the local interaction timescale, $dt = T_{\text{int}} \sim 30 \text{ Myr}$ for 47 Tuc as in Eq. 18, when the binary’s semi-major axis is a_0 . We remind the reader that at all times, the period of the BBH is no more than a few years and as the binary tightens its T_{int} increases.

Regarding the end of the evolution of the BBHs, we choose $a_{\text{end}} = 0.01 \text{ AU}$. This corresponds to 1.58 Myr until merger due to GW emission; a time much smaller than the Gyrs it takes for the binary to evolve.

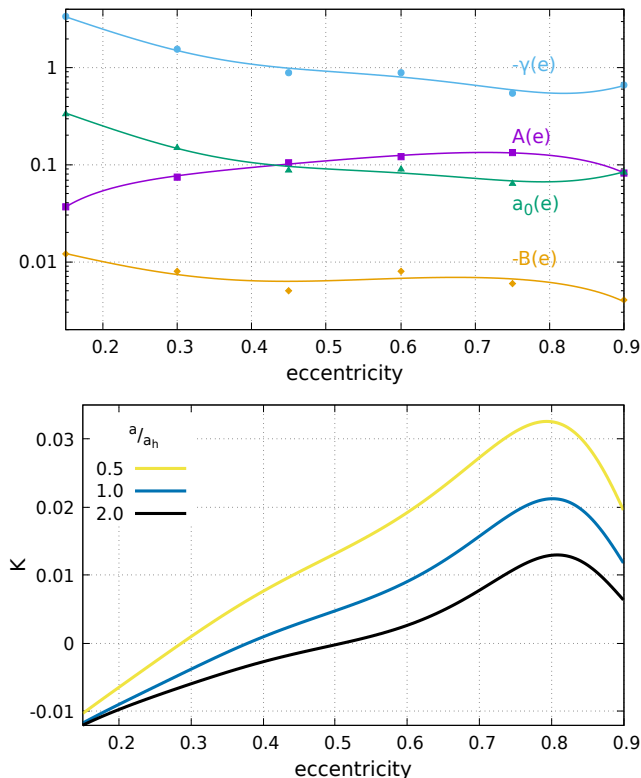


FIG. 6. *Top panel:* Cubic fits on the data (solid circles, squares, triangles and diamonds) in table 3 of [51] for $q = 1$. *Bottom panel:* The eccentricity growth rate $K(a, e) = A(e)(1 + a/a_0(e))^{\gamma(e)} + B(e)$ with the appropriate fitting parameters shown for three values of semi-major axis. Also, a_h is the hardness semi-major axis.

Appendix B: The ejection of binaries from globular clusters

In this appendix we make a short note on the ejection of a binary from a GC considering soft interactions. During each encounter of a binary $A - B$ with a third object C , on a statistical average the perturber acquires a high kick and by momentum conservation the binary

recoils. This recoil velocity is random and the distribution is spherically uniform. To a good approximation we can treat the binary as having its typical velocity dispersion in each encounter. By energy considerations one can show that the final relative velocity during the interaction of a binary $A - B$ with a third body C , is, [77],

$$\sigma_{A-B,C'} = \sqrt{\sigma_{A-B,C}^2 + 2 \frac{2}{\mu_{A-B,C}} \cdot \Delta E_b}, \quad (\text{B1})$$

where ΔE_b is given by Eq. 20. Assuming that $m_A + m_B \gg m_C$ we can estimate the recoil velocity, from momentum conservation, as, $v_{\text{recoil}} \approx \frac{m_C}{m_A + m_B} v_{A-B,C'}$. The binary will be kept in the cluster as long as the kick it acquires is not enough to eject it from the GC. The safest condition that the binary remains in the GC is that even if the recoil it acquires happens to be exactly opposite to its velocity with respect to the center of the GC it still has not surpassed the escape velocity threshold, i.e., $v_{\text{esc}} > v_{\text{kick}}^{\text{min}} = v_{\text{recoil}} - \sigma_{A-B,C}$, where we will use $v_{\text{esc}} = 2\sigma_{\text{star}}$ is the escape velocity. Finally, we obtain our condition for the critical semi-major axis to be, for $m_A = m_B = 10 M_{\odot}$ and $m_C = 1 M_{\odot}$,

$$a > a_{ej} \approx 0.0128 \times \left(\frac{H}{15}\right) \left(\frac{20 \text{ km/s}}{\sigma_{\text{star}}}\right)^2 \text{ AU}, \quad (\text{B2})$$

i.e. it should not be smaller than a critical value of roughly $a_{ej} \sim 10^{-2}$ AU at core radius in 47 Tuc. This value is only slightly bigger than a_{end} . Therefore, the binary's orbit is quite tight when it is ejected. We note again that these statements are valid in our context where BBHs mostly encounter $1 M_{\odot}$ stars and interact softly yet efficiently. If the BBH encounters another BH, the ejection point occurs at a larger semi-major axis, about $O(10)$ larger than our result, as in [53],

$$a_{ej} \simeq 0.266 \times \left(\frac{m_{\text{BH}}}{10 M_{\odot}}\right) \left(\frac{40 \text{ km/s}}{v_{\text{esc}}}\right)^2 \text{ AU}. \quad (\text{B3})$$